Journal of Materials Chemistry A

Accepted Manuscript

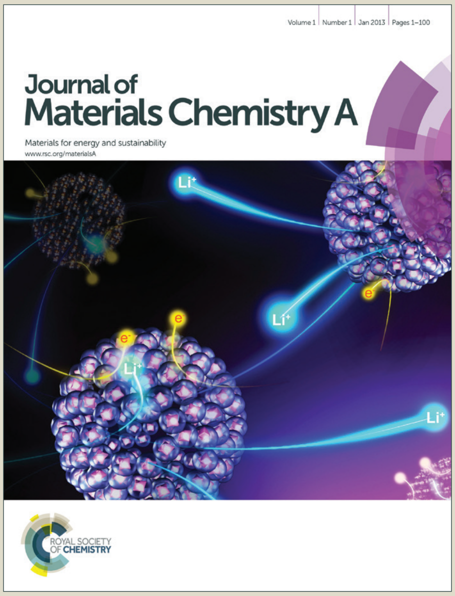

Trap-state Passivation of Titania Nanotubes by Electrochemical Doping for Enhanced Photoelectrochemical Performance

Lok-kun Tsui[1], Mikiko Saito[2], Takayuki Homma[2,3] and Giovanni Zangari[1,*]

[1]Department of Materials Science and Engineering and CESE, University of Virginia, Charlottesville, Virginia, 22904-4745, USA

[2]Institute for Nanoscience and Nanotechnology, Waseda University, Shinjuku-ku, Tokyo, 162-0041, Japan

[3]Department of Applied Chemistry, Waseda University, Okubo 3-4-1, Shinjuku, Tokyo 169-8555, Japan

Corresponding Author: Giovanni Zangari, Phone: 434-243-5474, Email: gz3e@virginia.edu

Table of Contents Entry

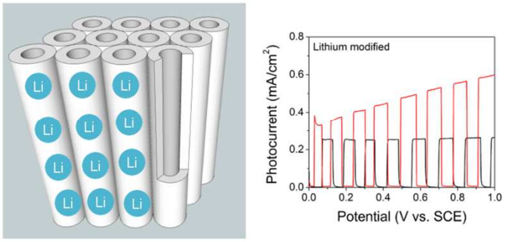

The photoelectrochemical performance of TiO_2 nanotubes was enhanced up to twofold by Li and H doping. This is due to reduced recombination coming from the doping's passivation of trap states.

Abstract

TiO_2 nanotubes are a widely investigated material for photoelectrochemical water splitting, but the presence of trap states limits their performance by facilitating the recombination of electron/hole pairs. In this investigation we unequivocally demonstrate that the photocurrent improvement observed in TiO_2 nanotubes after performing electrochemical doping with hydrogen or lithium ions is due to trap state passivation. Specifically, electrochemical impedance spectroscopy evidences that trap state defects disappear upon electrochemical doping, concurrent with an increase in electron lifetime and faster photocurrent transients. This results in a twofold enhancement in the photocurrent under simulated sunlight at 1.0 V vs. SCE. Li intercalation was confirmed and the structure as well as composition of the modified nanotubes was elucidated by GDOES, XPS, and TEM.

1. Introduction

Due to their unique combination of morphological, electronic, charge transport and environmental stability properties, TiO_2 nanotube arrays have been widely investigated as photoanodes for solar water splitting applications.[1–8] These materials are attractive also from a processing standpoint, since they can be simply and inexpensively formed by the anodization of Ti in F^- ion containing electrolytes.[9] The implementation of photoelectrochemical cells based on TiO_2 nanotube arrays however has been hampered so far by two main material limitations: the wide bandgap of 3.2 eV,[10] which limits the usable fraction of the solar spectrum to less than 5%, and the presence of various crystallographic and surface defects.[11–13] Defects in TiO_2 include not only beneficial shallow donors responsible for n-type doping in TiO_2 originating from O vacancies, but also trap states facilitating recombination, which originate from incompletely coordinated Ti^{4+} sites, Ti^{3+}, and surface OH groups.[11,13–17] The density of defect states has been recently shown to be dependent on synthesis conditions of the TiO_2 nanotubes.[18]

A possible approach to overcome at least one of these limitations is doping of TiO_2 nanotubes with hydrogen or lithium. Hydrogenation of TiO_2 nanoparticles at 200°C in a 20 bar H_2 atmosphere has been shown to form black TiO_2 exhibiting visible light photocatalysis.[19,20] A similar treatment on TiO_2 nanotubes resulted in efficient water splitting without an applied bias nor any catalyst.[21] Thermal processing at atmospheric pressure in air[22] or O_2 flow[23] yielded blue or black nanoparticles with visible light activity; annealing TiO_2 nanotubes in H_2 atmosphere in contrast yielded improved photoactivity but no visible absorption.[24] As an alternative to thermochemical methods, electrochemical doping has been utilized to incorporate Li or H into the TiO_2 lattice. In this process, a negative bias applied to TiO_2 in a suitable electrolyte containing Li^+ or H^+ ions results in ion intercalation in the lattice. Doping of TiO_2 nanotubes increases their conductivity,[25,26] enabling metal or semiconductor electroplating inside the tubes, and also changes their color, a phenomenon exploited in electrochromic devices.[25,27] In a different context, the electrochemical intercalation of Li in TiO_2 films or nanostructures has been investigated for Li-ion battery applications.[28–30] Loading levels of H or Li have been sparsely reported; under high pressure atmospheres, H can be loaded into TiO_2 up to a concentration of 1-3 wt%, corresponding to a molar H:Ti ratio of 0.8-2.4.[31,32] Anatase TiO_2 on the other hand can accommodate a Li concentration corresponding to Li:Ti = 0.27-0.5.[29,33,34] Ion intercalation into the lattice of TiO_2 generally leads to the reduction of Ti^{4+} to Ti^{3+} according to (Equations 1-2),[25,26]

$$\mathrm{Ti(IV)O_2 + Li^+ + e^- \rightarrow LiTi(III)O_2} \qquad (1)$$

$$\mathrm{Ti(IV)O_2 + H^+ + e^- \rightarrow HTi(III)O_2} \qquad (2)$$

which has been claimed to be responsible for visible light activity and improved photoelectrochemical performance. Some reports claim both effects,[19–23] while others observe exclusively an increase in photocurrent,[14,24,35] which suggests that the structural modifications induced by the various methods described above differ in a subtle manner and may contribute differently to changes in the electronic structure,[19,22] charge carrier transport,[14] or catalytic activity.[21]

Meekins[14] and Kang[35] for instance investigated the electrochemical doping of TiO_2 and found no visible light response associated to doping; these two studies suggested that the enhancement in photoelectrochemical response could be associated with the passivation of trap states in TiO_2.

The evidence for trap state passivation however was indirect, through the detection of longer electron lifetimes[14] and a decreased intensity of photoluminescence;[35] a direct inspection of the defect structure in doped TiO_2 and a validation of the above hypothesis has not yet been reported.

In this paper, we report on the enhancement in photoelectrochemical performance of TiO_2 nanotubes via electrochemical modification of TiO_2 by Li and H, and we demonstrate that this effect is due to *trap state passivation*. Specifically, electrochemical impedance spectroscopy is used to determine the energy level and density of defect states, showing that the traps are no longer detectable after hydrogen or lithium doping. As a consequence, we assign the enhanced performance to trap state passivation, which limits recombination and enhances the electron lifetime. Additional characterization by GDOES, XPS, and high resolution TEM are used to further investigate the spatial extent and character of doping inside the TiO_2 nanotubes.

2. Results and Discussion

The crystal structure of TiO_2 nanotubes does not change upon electrochemical intercalation, as determined by Raman spectroscopy and x-ray diffraction (Supporting Information, Figure S1). Figure 1 shows the high resolution TEM images obtained on TiO_2 nanotubes before and after Li doping. As-made nanotubes exhibit well defined atomic lattice fringes at the edge of the walls, while TiO_2 nanotubes modified by Li doping display a darker surface region at the wall edge, 7 nm in thickness, lacking well defined lattice fringes. The lattice parameters were extracted from this region by FFT analysis (see SI Figure S2 for calculated diffraction patterns), and values of c = 0.94 nm and a = 0.37 nm were obtained, matching the standard values of anatase TiO_2 (PDF 01-071-1166).[36] The difference in contrast suggests the presence of somewhat different structures in the surface and subsurface regions; the uniformity of the lattice constant however does not support this notion. If Li intercalation occurs in the surface region, the measured lattice constants indicate that intercalation would induce little or no deformation in the crystal lattice of TiO_2. The reported volume change upon lithium ion intercalation however is at most a 7% expansion in the lattice parameters and a 4% volume expansion of the TiO_2 unit cell;[34,37,38] this variation is difficult to detect in TEM images. The increased width of the diffraction peaks (see Figure S2(e-f)) upon Li doping however evidences the introduction of some strain, which we assign to the intercalation process.

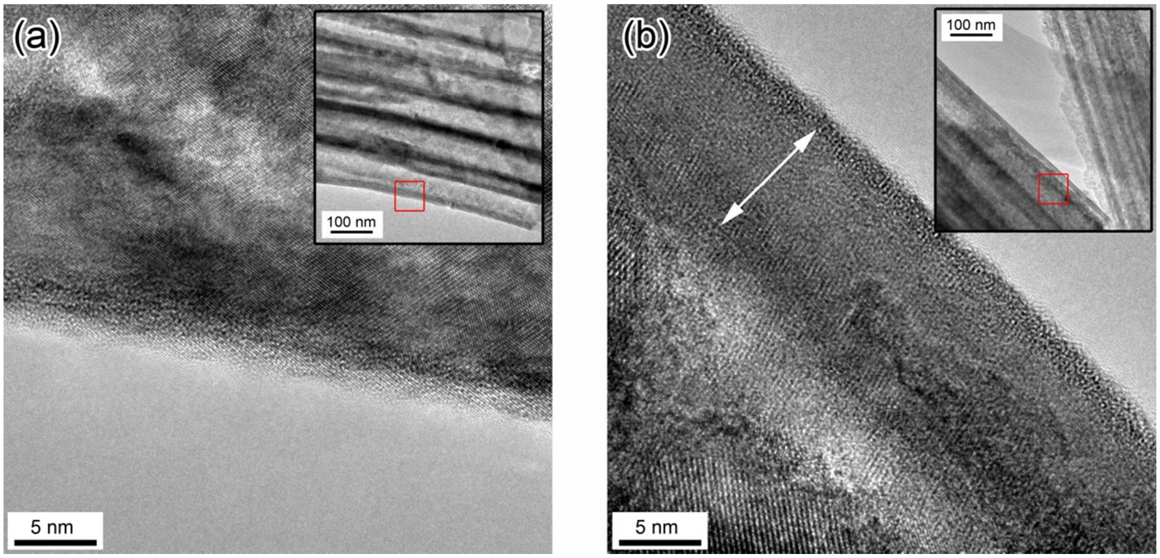

Figure 1. High resolution TEM images of (a) undoped and (b) Li doped TiO_2 nanotubes. Inset in each region is a lower magnification TEM image of each location.

The concentration of H or Li in electrochemically modified TiO_2 nanotubes was analyzed by GDOES. Since this method involves the simultaneous removal of material from the nanotube array from all the exposed surfaces during generation of the plasma, only an overall dopant fraction could be obtained; the measured value could also be affected by detection of material being expelled from the substrate. GDOES detected Li within the Li-doped TiO_2 nanotubes, but the hydrogen level was the same in the H-doped and untreated TiO_2 nanotubes. In order to quantitatively assess Li content, the integral of the Li and O atomic fraction detected as a function of sputtering time was computed. Assuming an O:Ti ratio of 2:1 for TiO_2, the average Li fraction within the nanotubes was determined to be 0.72%. With regard to the H concentration, we were unable to obtain a detectable difference among the various samples; this may be due to the H fraction being below 0.1 at% and therefore limited by the detection capability of this instrument. High resolution XPS spectra in the Ti 2p region for the three samples are plotted in Figure 3. Two peaks are observed associated with the Ti 2p states,[39] and only a small shift by about 0.5-1.0 eV towards higher binding energies is observed after Li doping. According to the intercalation model summarized in Eqns. (1) and (2), doping should be accompanied by reduction of a fraction of the Ti^{4+} sites to Ti^{3+}. A peak associated with the formation of Ti^{3+} upon Li intercalation at a concentration of $Li_{0.32}TiO_2$ has been observed by Södergren et al. and indicated in Fig. 2 at 456 eV;[40] no peaks are however seen at this energy. It is possible that the limited fraction of Li intercalated into Ti may render the detection of the Ti^{3+} state by XPS impossible. In the case of H doping, Chen's black TiO_2 formed by annealing in high pressure H_2 atmospheres did not contain any other chemical states than Ti^{4+}, but the same shoulder that Södergren et al. found was observed after UV illumination.[20] Our results appear consistent with the XPS spectra obtained by Liu for H and by Kang for Li; [21,35] in the latter work, the authors did not detect the formation of additional peaks associated with Ti^{3+} even with an extended Li intercalation time of 5 min.[35]

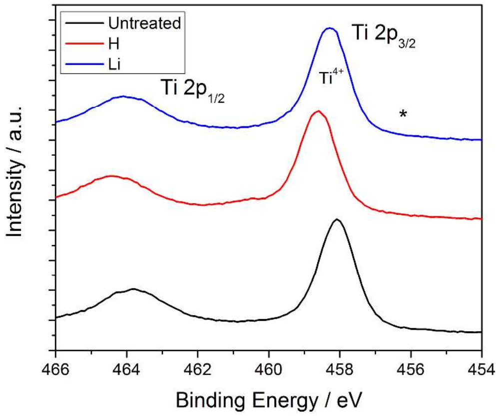

Figure 2. XPS spectra of TiO_2 nanotubes unmodified and doped. (*) indicates the expected position of Ti^{3+} when significant Li intercalation occurs.

Figure 3 (a-b) compares the photocurrents under simulated sunlight of the TiO_2 nanotubes modified with Li or H with those of the unmodified TiO_2 ones. Qualitatively, the photocurrent is saturated between 0.1 and 1 V_{SCE} in the unmodified nanotubes, while it increases gradually in both modifications, such that under an applied bias of 1.0 V_{SCE}, the photocurrent in the modified nanotubes is up to two times as large as the unmodified ones. Photocurrent saturation under anodic bias has been ascribed to the increase in the depth of the space charge layer, reaching its maximum possible value when it attains the thickness of the nanotube walls.[41] The fact that no geometric changes are seen in the tubes upon doping suggests that photocurrent saturation may not be due to space charge layer limitations, but to Fermi level pinning linked to a high density of defect states. We propose therefore that in the modified nanotubes an unpinning of the Fermi-level is occurring due to the passivation of these trap states, while Fermi-level pinning by defects in unmodified tubes would result in photocurrent saturation under bias.[42] The thickness of the space charge layer L_{SC} can be readily calculated when the density of dopants and the dielectric constant for TiO_2 are known,[43] resulting in a value of 15 nm under a 2V applied bias vs. flat band potential (Supplementary Information, Figure S3), which is half the nanotube wall thickness of 30-35 nm. The flat band potential of these TiO_2 nanotubes is located at -0.2 V_{SCE}.[18,44] If the space charge layer expands from both sides, the potential at which it is maximized should occur near 1.8 V_{SCE}, well above the potential where the photocurrent saturates in Figure 3(a).

To address the possibility that doping of TiO_2 with Li or H may induce a photoelectrochemical response under visible light, measurements of photocurrent spectra comparing undoped and doped TiO_2 nanotube samples are plotted in Figure 3 (c), showing that no photocurrent is generated at wavelengths above ~400 nm. This corresponds roughly to the 3.2 eV bandgap of anatase TiO_2, which absorbs only light with wavelengths below 387.5 nm. At the same potential where the IPCE measurements were taken (0.5 V_{SCE}), the improvement under simulated sunlight is 1.4x, which is completely accounted for by the 1.4x increase in IPCE in the UV range. After electrochemical doping with Li or H a brief transition to a black color is observed, but this dissipates within 30 seconds after the sample has been rinsed and dried. This is in contrast with the observation of permanent color change under thermochemical modification conditions,[19,21–23] and suggests that electrochemical H or Li doping of TiO_2 does not cause a permanent change in the band gap; the observed enhancement of the photocurrent response should be therefore associated only with trap state passivation. If this were the case, a decrease in recombination rate should be observed; this could be indeed confirmed by monitoring the open circuit voltage decay,[14,45] which directly correlates with the electron lifetime through Equation 3:

$$\tau = \frac{k_B T}{e}\left(\frac{dV_{OCV}}{dt}\right)^{-1} \qquad (3).$$

In this equation, k_B is Boltzmann's constant, T is temperature in Kelvin, and e is the electron charge. The results are displayed in Fig. 4, which shows an increase in the electron lifetime at 0.2 V_{SCE} by a factor of 20 for hydrogen doping and a factor of 2 after lithium doping. The increase in electron lifetime does not scale with the photocurrent, suggesting that other effects, such as the binding energy of electrons at these defect sites, may affect the trapping time and contribute to the observed effects.

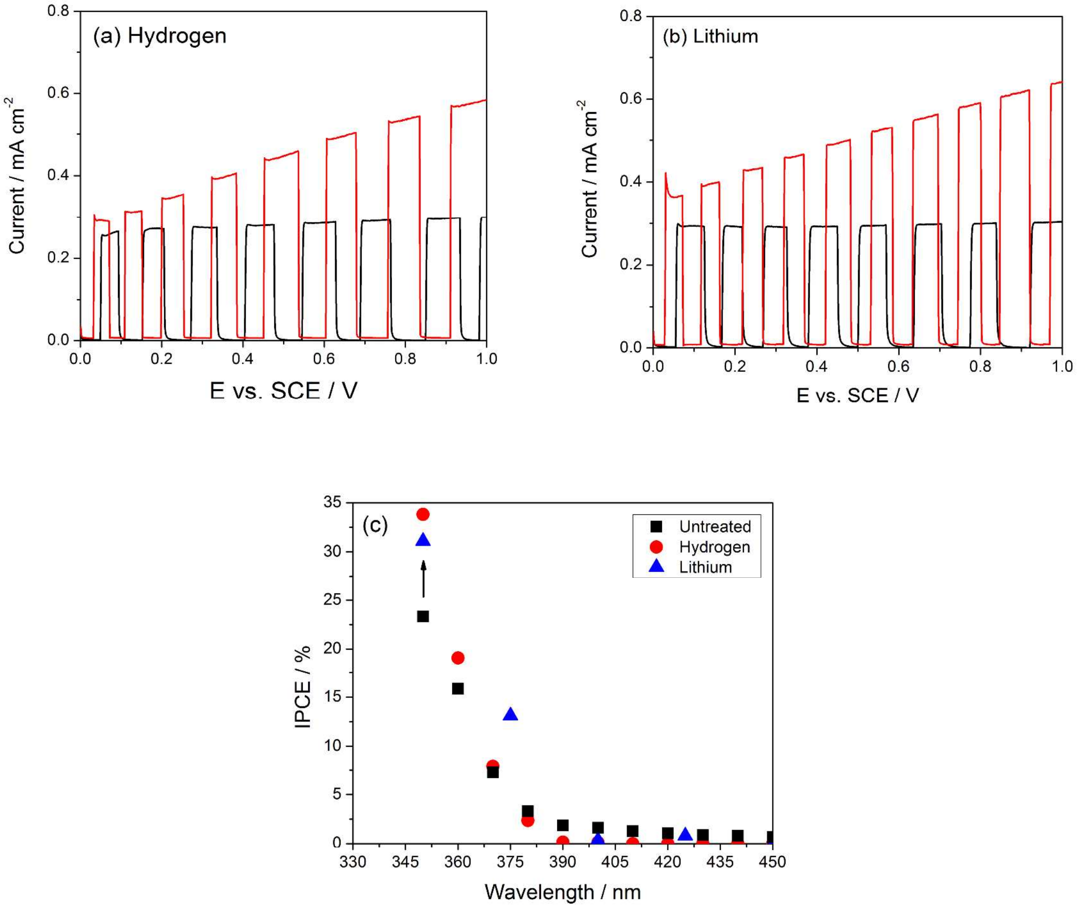

Figure 3. Photoelectrochemical measurements of TiO_2 nanotubes modified (dashed lines) by (a) Hydrogen and (b) Lithium show up to a twofold enhancement under simulated sunlight. (c) IPCE spectra shows that doping does not induce photoelectrochemical reactions under visible light illumination.

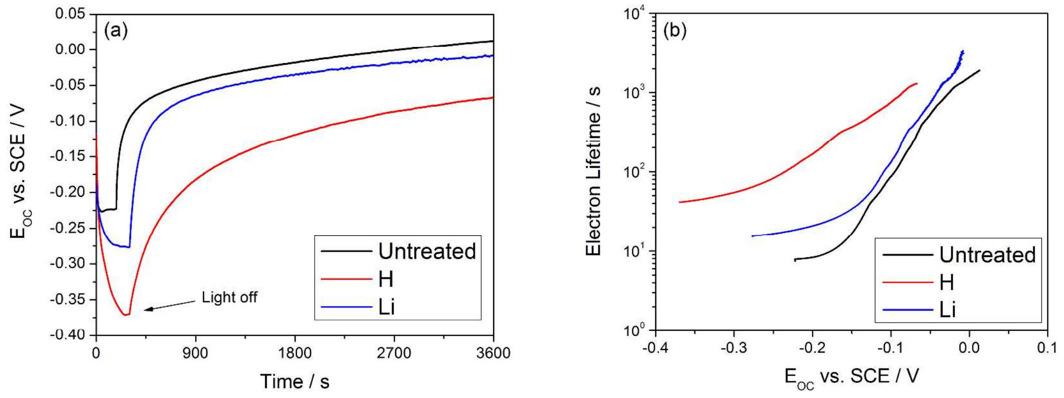

Figure 4. (a) OCV decay of TiO_2 nanotubes following the switching off of UV light. (b) Calculated electron lifetime is improved by a factor of 20 for hydrogen and a factor of 2 for lithium.

Electrochemical impedance spectroscopy and photocurrent transients were used to further investigate the trap passivation mechanism. To extract the density and energy level of crystalline defects, we obtained the interface capacitance (C_p) in the low frequency limit using equation 4 (Figure 6).[47,48] In this equation, ω is the angular frequency, Im(Z) is the imaginary portion of the impedance, Re(Z) is the real portion of the impedance, and R_Ω is the Ohmic resistance determined in the high frequency limit.

$$C_P(\omega) = -[\omega * Im(Z)(1 + D^2)]^{-1} \tag{4}$$

$$D \equiv \frac{\mathrm{Re(Z)} - \mathrm{R}_\Omega}{-\mathrm{Im(Z)}}$$

Two peaks are observed in the unmodified TiO_2 nanotubes, located at -0.2 and 0.4 V_{SCE} and associated with shallow dopant states and deep level trap states, respectively.[18] After H or Li doping the peak corresponding to the deep levels is no longer detectable in the capacitance scan (Figure 5a), except for a flat background which increases by an order of magnitude in the positive potential (deep states) region. The increase in capacitance due to Li doping has been associated with an increase in the dielectric constant, up to 500-900 for heavily Li doped TiO_2,[34] and hydrogenation has also been shown to increase the capacitance of TiO_2 by 40 times.[49] Van de Krol et al. claim that the increase of the dielectric constant may originate from an increase in the polarizability of TiO_2 from intercalated Li ions.[34] The evidence for trap state passivation is further supported by the photocurrent onset transients. In polycrystalline TiO_2 nanotubes exhibiting a high density of trap states, a slow onset transient is associated with photogenerated charges initially being used for trap filling and later contributing to the observed steady state current density (Figure 5b).[50] Our calculations have placed the density of trap states associated with trap filling within an order of magnitude of the density of defects calculated with the frequency dependent capacitance, which strongly suggests that these trap states are responsible for the slow onset transients.[44] After H or Li doping, the response to simulated sunlight illumination is much sharper and indicates very low losses associated to the capture of electrons by trap states (Figure 5b).

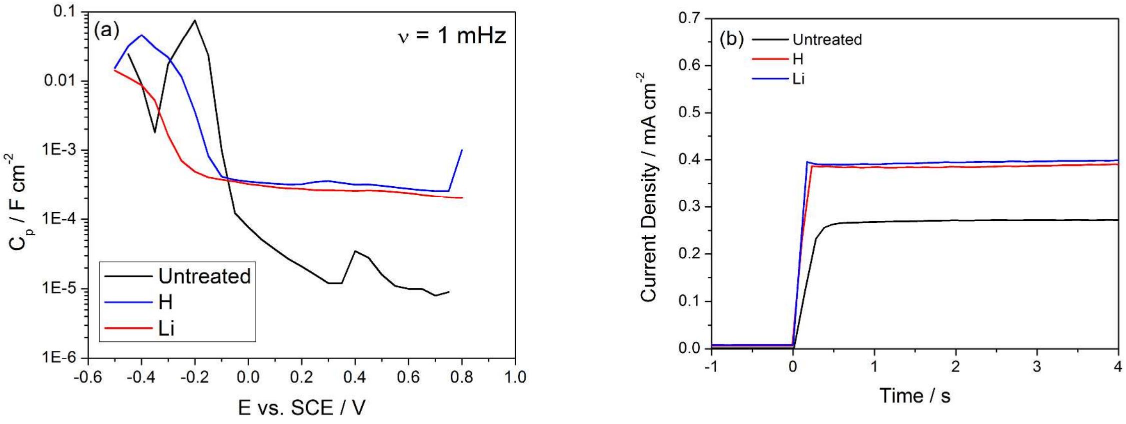

Figure 5. (a) Frequency dependent capacitance at 1 mHz as a function of potential. A peak is evident centered at 0.4 V_{SCE} associated with deep level trap states before doping. No peak is detected after doping though an increase in overall background capacitance is observed. (b) Photocurrent onset transients show that the response to illumination is slow in undoped TiO_2 and fast in doped TiO_2 nanotubes.

Electrochemical impedance spectroscopy under UV light illumination was also used to probe the kinetics of the photoelectrochemical reaction, which we assume to be water splitting. Figure 6(a) shows the impedance response plotted in the Nyquist representation. A transmission line model (Figure 6(a), Inset) was used to obtain the charge transfer resistance R3,[18,51] and the results are plotted in Figure 6(b). R3 under light is observed to drop by one order of magnitude after illumination, indicating improvements in the kinetics of the water splitting reaction. We do not attribute this to a catalytic effect of the doping process; rather, we hypothesize that more holes are available since they were not lost to recombination, resulting in an increased rate of the water splitting reaction.

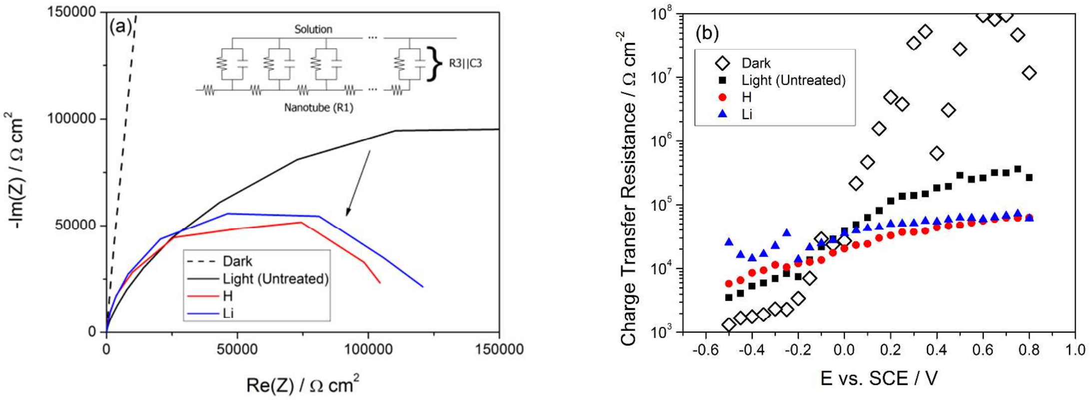

Figure 6. (a) Impedance spectra of TiO_2 nanotubes in the dark and under UV illumination at +0.3 V_{SCE}. Inset: Transmission line equivalent circuit model used to fit the impedance. (b) Calculated charge transfer resistance of TiO_2 nanotubes drops by a factor of 10 at potentials positive of $0.2V_{SCE}$ after H and Li doping.

Taking the density of trap states to be 9.7 x 10^{16} cm^{-3}, as reported in ref. [18], the density of Li or H that must be incorporated into TiO_2 for complete trap state passivation can be calculated. The density of anatase TiO_2 is 3.99 g cm^{-3}, and its molar mass is 79.866 g mol^{-1}.[52] Therefore, the density of Ti atoms is 3.01 x 10^{22} cm^{-3}. Dividing trap density by the density of Ti atoms and assuming a one-electron reduction of a Ti^{4+} site to Ti^{3+}, the fraction of Ti that must be reduced for complete trap state passivation is 3.22 x 10^{-6}.[14] As discussed above, this is five orders of magnitude smaller than the theoretical upper limit of Li intercalation at a stoichiometry of $Li_{0.5}TiO_2$. Even if a substantial portion of the Li/H diffuses out of TiO_2, which could explain the transient nature of the electrochromism in the nanotubes, it is hypothesized that enough remains to retain the effect of photoelectrochemical enhancement. Adding more Li to the nanotubes by increasing the reduction time is found to have no effect (Supplementary Information, Figure S4). Numbers for the density of electrochemically intercalated H are not available, but this would also be several orders of magnitude smaller than the upper stoichiometry of $H_{0.8\text{-}2.4}TiO_2$ observed in thermochemically doped materials. We observe that in both H and Li modified TiO_2, the performance enhancement is the same; this is in contrast to literature reports, showing that Li performs better.[14] H and Li are both expected to readily incorporate into the interstitials sites formed by the voids within the octahedrons of the anatase TiO_2 structure.[20,32,34,53] If the underlying cause of the photocurrent enhancement is the trap state passivation that accompanies reactions in Eqns. (1) and (2) and both H and Li are located at similar sites there is no reason to expect that H and Li modified nanotubes would perform differently.

We may also estimate the depth of intercalation *d* by using a modified form of Faraday's Law to determine the fraction of TiO_2 that is being reduced (Equation 5). This calculation should only be valid for Li, where relatively few bubbles are observed during intercalation, and not for H, where a substantial portion of the current density during H doping would go towards hydrogen evolution, associated with vigorous gas generation at the electrode. If Q is the total charge passed, z is the number of electrons (1 for Ti^{4+} reduction), M is the molar mass of TiO_2 (79.866 g mol^{-1}), F is Faraday's Constant (96485 C mol^{-1}), ρ is the density of anatase TiO_2 (3.99 g cm^{-3}),[52] and x is a scaling constant based on the ratio of Li to Ti, then

$$\mathrm{d} = \frac{\mathrm{Q}\mathrm{M}_{\mathrm{TiO_2}}}{\mathrm{z}\mathrm{F}\rho_{\mathrm{TiO_2}}\mathrm{x}} \qquad (5).$$

A one-dimensional semi-infinite uniform block of lithiated TiO_2 is assumed, with Li intercalation occurring at the surface. For every unit length of TiO_2, only a fraction of the Ti^{4+} atoms can be reduced to Ti^{3+} to accommodate Li. Let's assume that at the surface TiO_2 accommodates Li to a stoichiometry of $Li_{0.5}TiO_2$, thus calculating a lower bound on the minimum penetration of lithiation. Under this assumption, for a given length only half the Ti atoms may be reduced, such that x = 0.5. With a charge passed of 1.70×10^{-3} C cm^{-2}, which corresponds to 3 s of applied cathodic potential, a layer of $Li_{0.5}TiO_2$ would exhibit an intercalated depth of 7.1 nm. This is close to the thickness of the dark area observed in high resolution TEM images in Figure 1. Van de Krol estimates that the maximum extent of lithiation could be up to 17 nm, placing this thickness within the thickness limit imposed by diffusion of Li in TiO_2.[34]

Finally, two issues regarding the durability of the doping process were considered: the stability of a sample over extended periods of storage and the stability of the Li dopant in neutral electrolytes. The stability of the doping process was studied by recording the photocurrent before and after 1 month of sample storage in ambient air. In Figure 7(a), we show the photocurrent of an H doped sample at 1.0 V_{SCE} to be 0.57 mA cm^{-2} before storage and 0.47 mA cm^{-2} after storage, corresponding to a decrease of only 20% after 1 month. Kang et al. have raised the issue of the stability of Li in neutral electrolytes, claiming that doping before annealing the TiO_2 nanotubes is necessary to maintain the doping effects.[35] Figure 7(b) shows the current transient under potentiostatic bias of 0.5 $V_{SCE;}$ less than 0.05 mA cm^{-2} decrease in the photocurrent is observed over 900 seconds. These results are in direct contrast to ref. [35], which showed no enhancement with Li doping in neutral electrolytes.

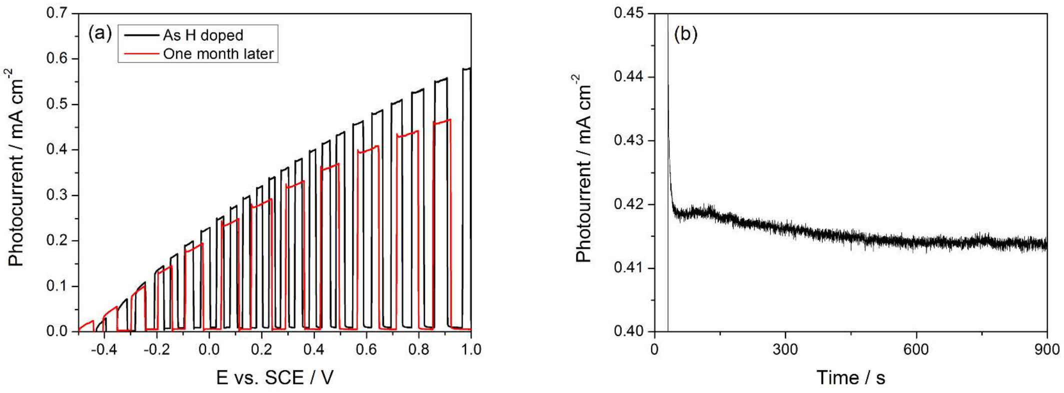

Figure 7. (a) Stability of H doped TiO_2 NTs after prolonged storage. (b) Photocurrent transient of Li doped TiO_2 showing stability over 15 minutes.

3. Experimental Section

TiO_2 nanotubes were produced by a two-stage anodization method[44], using a Kepco BOP-100 power supply controlled with LabVIEW®. Ti foils (Alfa Aesar, 99+%, annealed, metals basis) were first cleaned by sequentially sonicating in acetone, isopropanol, and methanol, 30 minutes for each step. An electrical connection to each 2 cm × 0.7 cm × 0.127 mm Ti foil was made by spot welding a Ni wire to the top edge. The nanotubes were anodized in a two electrode configuration with a Pt mesh as the counter electrode, in an electrolyte containing 0.3 wt% NH_4F and 2 vol% H_2O (Millipore) in ethylene glycol at 50V. The first anodization was carried out for 1 hour to form a ~10 µm layer of nanotubes; this layer was then loosened by sonication in water for 30 minutes and removed with adhesive tape. In the second step, the nanotubes were anodized for 5 additional minutes in the same conditions to obtain highly uniform arrays of TiO_2 nanotubes, 1 µm in length. The TiO_2 nanotubes were finally annealed in air at 350°C to convert amorphous TiO_2 to anatase TiO_2.[54]

Hydrogen and lithium modification of TiO_2 nanotubes were carried out in 0.5 M H_2SO_4 or 1M $LiClO_4$, respectively, with an applied potential of -1.55 V_{SCE} for 3s. Photocurrent measurements were carried out in a solution of 0.2M Na_2SO_4 and 0.1M $NaCH_3COO$ (pH = 7), in the potential range of 0 to 1.0 V_{SCE}. This range was selected to avoid inadvertent doping during photocurrent testing. The light source was an Oriel Sol 1A solar simulator emitting AM 1.5 simulated sunlight with an intensity of 100 mW cm^{-2}. Electrochemical impedance spectroscopy (EIS) measurements were carried out in the dark at potentials between 0.5 to -0.5 V_{SCE} and in a frequency range from 200 kHz to 1 mHz with an amplitude of 20 mV. Under these same conditions, EIS was also carried out under the illumination of a 0.4 mW UV LED (Lumex SSL-LXTO46365 C, λ = 363-370 nm); the resulting spectra were fitted to a transmission line equivalent circuit model.[18,51] Open circuit voltage decay was measured by holding the samples under UV-LED illumination for 5 minutes at OCV, and then monitoring the voltage decay as a function of time. For these electrochemical measurements, a Pt mesh counter electrode, a saturated calomel reference electrode (SCE), and a BioLogic SP-150 potentiostat were used.

Transmission electron microscope (TEM) images of TiO_2 nanotubes were obtained by scratching with a razor blade several 3×3 mm^2 Ti foils with TiO_2 nanotubes, and collecting the resulting debris in a glass vial containing 2 mL of ethanol. This suspension was sonicated for 30 minutes, resulting in the ethanol to take on a pale white color. A lacy carbon TEM grid (Ted Pella) was then immersed into the ethanol-nanotube suspension and then dried under an incandescent lamp. This dipping and drying process was repeated for a total of 10 times to allow at least one fragment of the TiO_2 nanotube array to appear in each grid window. High-resolution TEM images were obtained with an FEI Titan TEM. Glow discharge optical emission spectrometry and XPS measurements were performed on TiO_2 nanotube array samples of 2×2 cm^2 in size prepared as described above. A glow discharge optical emission spectrometer (GDOES, JY-5000RF, HORIBA) was used to investigate the H or Li content of the TiO_2 nanotubes. The sampling area was 4 mm diameter. Depth profiling was carried out at an argon pressure of 600 Pa, at a power of 35 W. A X-ray photoelectron spectroscopy (XPS, JPS-9010TR, JEOL Ltd.) measurement was performed to determine the oxidation state of Ti. The radiation source was MgKα and the measurement was carried out at 10 kV, 10 mA. The sampling area was 7 mm in diameter. The XPS spectra were calibrated to the peak of C 1s.

4. Conclusion

We have studied the structural changes, the mechanism and the increase in photoelectrochemical performance of 1 μm long TiO_2 nanotubes upon H or Li doping, showing that the two treatment methods are equally effective and can produce up to a 200 % improvement in the photocurrent under simulated sunlight at 1.0 V_{SCE}. EIS and photocurrent transients prove that performance enhancement is due to trap state passivation, suggesting new avenues to further tailor properties. Our measurements have confirmed that Li is present in sufficient amounts to be detected by GDOES, but small enough that the hypothesized Ti^{3+} chemical state cannot be resolved using XPS. Calculations show that minute amounts of Li and H are sufficient to passivate the trap states in TiO_2, explaining why extended intercalation times reported in the literature do not provide further enhancements.

Acknowledgments

We acknowledge the support of the ARCS Foundation and from the National Science Foundation Grant No. CMMI-1229603.

Supporting Information

Raman spectra, XRD patterns, FFTs of HR-TEM images, calculation of the thickness of the space charge layer, and influence of Li doping time are available as supporting information.

References

1. C. Das, P. Roy, M. Yang, H. Jha, and P. Schmuki, *Nanoscale*, 2011, **3**, 3094–6.
2. Z. Zhang, X. Yang, M. N. Hedhili, E. Ahmed, L. Shi, and P. Wang, *ACS App. Mater. Interfaces*, 2014, **6**, 691–6.
3. B. Chen, J. Hou, and K. Lu, *Langmuir*, 2013, **29**, 5911–9.
4. A. Mazare, I. Paramasivam, K. Lee, and P. Schmuki, *Electrochem. Comm.*, 2011, **13**, 1030–1034.
5. Q. Kang, J. Cao, Y. Zhang, L. Liu, H. Xu, and J. Ye, *J. Mater. Chem. A*, 2013, **1**, 5766.
6. M. Altomare, K. Lee, M. S. Killian, E. Selli, and P. Schmuki, *Chemistry (Easton).*, 2013, **19**, 5841–4.
7. J. Tang, J. R. Durrant, and D. R. Klug, *J. Amer. Chem. Soc.*, 2008, **130**, 13885–91.
8. L. -k. Tsui and G. Zangari, *J. Electrochem. Soc.*, 2014, **161**, D3066–D3077.
9. P. Roy, S. Berger, and P. Schmuki, *Angew. Chemie (Int. ed. Eng.)*, 2011, **50**, 2904–39.
10. L. Kavan, M. Grätzel, S. E. Gilbert, C. Klemenz, and H. J. Scheel, *J. Amer. Chem. Soc.*, 1996, **118**, 6716–6723.
11. T. Berger, M. Sterrer, O. Diwald, E. Knözinger, D. Panayotov, T. L. Thompson, and J. T. Yates, *J. Phys. Chem. B*, 2005, **109**, 6061–8.
12. C. P. Kumar, N. O. Gopal, T. C. Wang, M.-S. Wong, and S. C. Ke, *J. Phys. Chem. B*, 2006, **110**, 5223–9.
13. A. Hagfeldt, H. Lindström, S. Södergren, and S.-E. Lindquist, *J. Electroanal. Chem.*, 1995, **381**, 39–46.
14. B. H. Meekins and P. V. Kamat, *ACS Nano*, 2009, **3**, 3437–46.
15. B. J. Morgan and G. W. Watson, *Phys. Rev. B.*, 2009, **80**, 2–5.
16. S. A. Ali Yahia, L. Hamadou, A. Kadri, N. Benbrahim, and E. M. M. Sutter, *J. Electrochem. Soc.*, 2012, **159**, K83.

17. S.-C. Ke, T.-C. Wang, M.-S. Wong, and N. O. Gopal, *J. Phys. Chem. B*, 2006, **110**, 11628–34.

18. L. Tsui and G. Zangari, *Electrochim. Acta*, 2014, **121**, 203–209.

19. X. Chen, L. Liu, P. Y. Yu, and S. S. Mao, *Science (80-.).*, 2011, **331**, 746–50.

20. X. Chen, L. Liu, Z. Liu, M. a Marcus, W.-C. Wang, N. a Oyler, M. E. Grass, B. Mao, P.-A. Glans, P. Y. Yu, J. Guo, and S. S. Mao, *Sci. Rep.*, 2013, **3**, 1510.

21. N. Liu, C. Schneider, D. Freitag, M. Hartmann, U. Venkatesan, J. Müller, E. Spiecker, and P. Schmuki, *Nano Lett.*, 2014, **14**, 3309–13.

22. F. Zuo, L. Wang, T. Wu, Z. Zhang, D. Borchardt, and P. Feng, *J. Am. Chem. Soc.*, 2010, **132**, 11856–7.

23. A. Naldoni, M. Allieta, S. Santangelo, M. Marelli, F. Fabbri, S. Cappelli, C. L. Bianchi, R. Psaro, and V. Dal Santo, *J. Am. Chem. Soc.*, 2012, **134**, 7600–3.

24. D. Wang, L. Liu, F. Zhang, K. Tao, E. Pippel, and K. Domen, *Nano Lett.*, 2011, **11**, 3649–55.

25. R. Hahn, A. Ghicov, H. Tsuchiya, J. M. Macak, A. G. Muñoz, and P. Schmuki, *phys. stat. sol.*, 2007, **204**, 1281–1285.

26. J. M. Macak, B. G. Gong, M. Hueppe, and P. Schmuki, *Adv. Mater.*, 2007, **19**, 3027–3031.

27. A. Ghicov, H. Tsuchiya, R. Hahn, J. M. Macak, A. G. Muñoz, and P. Schmuki, *Electrochem. Comm.*, 2006, **8**, 528–532.

28. Q. L. Wu, J. Li, R. D. Deshpande, N. Subramanian, S. E. Rankin, F. Yang, and Y. Cheng, *J. Phys. Chem. C*, 2012, **116**, 18669–18677.

29. K. H. Reiman, K. M. Brace, T. J. Gordon-Smith, I. Nandhakumar, G. S. Attard, and J. R. Owen, *Electrochem. Comm.*, 2006, **8**, 517–522.

30. W. Wei, G. Oltean, C.-W. Tai, K. Edström, F. Björefors, and L. Nyholm, *J. Mater. Chem. A*, 2013, **1**, 8160.

31. P. Raghunath, W. F. Huang, and M. C. Lin, *J. Chem. Phys.*, 2013, **138**, 154705.

32. C. Sun, Y. Jia, X.-H. Yang, H.-G. Yang, X. Yao, G. Q. (Max) Lu, A. Selloni, and S. C. Smith, *J. Phys. Chem. C*, 2011, **115**, 25590–25594.

33. M. Wagemaker, W. J. H. Borghols, and F. M. Mulder, *J. Amer. Chem. Soc.*, 2007, **129**, 4323–7.

34. R. van de Krol, A. Goossens, and J. Schoonman, *J. Phys. Chem. B*, 1999, **103**, 7151–7159.

35. U. Kang and H. Park, *Appl. Catal. B Environ.*, 2013, **140-141**, 233–240.

36. International Centre for Diffraction Data, ICDD DDView+, version 4.8.0.5, Newtown Square, PA, USA, 2009.

37. R. J. Cava, A. Santoro, D. W. Murphy, S. M. Zahurak, R. M. Fleming, P. Marsh, and R. S. Roth, *J. Solid State Chem.*, 1986, **65**, 63–71.

38. R. Van De Krol, A. Goossens, and E. A. Meulenkamp, 1999, **146**, 3150–3154.

39. H. G. Yang and H. C. Zeng, *J. Phys. Chem. B*, 2004, **108**, 3492–3495.

40. S. Södergren, H. Siegbahn, H. Rensmo, H. Lindström, A. Hagfeldt, and S. Lindquist, *J. Phys. Chem. B*, 1997, **101**, 3087–3090.

41. R. Beranek, H. Tsuchiya, T. Sugishima, J. M. Macak, L. Taveira, S. Fujimoto, H. Kisch, and P. Schmuki, *Appl. Phys. Lett.*, 2005, **87**, 243114.

42. A. J. Bard, A. B. Bocarsly, F. R. F. Fan, E. G. Walton, and M. S. Wrighton, *J. Amer. Chem. Soc.*, 1980, **102**, 3671–3677.

43. G. K. Boschloo, *J. Electrochem. Soc.*, 1997, **144**, 1311.

44. L. Tsui, T. Homma, and G. Zangari, *J. Phys. Chem. C*, 2013, **117**, 6979–6989.

45. A. Zaban, M. Greenshtein, and J. Bisquert, *Chemphyschem*, 2003, **4**, 859–64.

46. C. A. Grimes, *J. Mater. Chem.*, 2007, **17**, 1451.

47. G. Oskam, P. P. M. Hoffmann, and P. P. C. Searson, *Phys. Rev. Lett.*, 1996, **76**, 1521–1524.

48. G. Oskam, J. C. Schmidt, P. M. Hoffmann, and P. C. Searson, *J. Electrochem. Soc.*, 1996, **143**, 2531.

49. X. Lu, G. Wang, T. Zhai, M. Yu, J. Gan, Y. Tong, and Y. Li, *Nano Lett.*, 2012, **12**, 1690–6.

50. K. Schwarzburg and F. Willig, *Appl. Phys. Lett.*, 1991, **58**, 2520.

51. J. Bisquert, G. Garcia-Belmonte, F. Fabregat-Santiago, N. S. Ferriols, P. Bogdanoff, and E. C. Pereira, *J. Phys. Chem. B*, 2000, **104**, 2287–2298.

52. W. H. D. Lide, Ed., in *CRC Handbook of Chemistry & Physics*, Taylor and Francis Group, LLC, Boca Raton, FL, 94th edn., 2014, pp. 4–96.

53. B. Zachau-Christiansen, K. West, T. Jacobsen, and S. Atlung, *Solid State Ionics*, 1988, **30**, 1176–1182.

54. A. Tighineanu, T. Ruff, S. P. Albu, R. Hahn, and P. Schmuki, *Chem. Phys. Lett.*, 2010, **494**, 260–263.